SAFIR-3000 Lightning Statistics over the Beijing Metropolitan Region during 2005–07

FAN WU

Key Laboratory of Cloud-Precipitation Physics and Severe Storms, Institute of Atmospheric Physics, Chinese Academy of Sciences, and University of Chinese Academy of Sciences, Beijing, China

XIAOPENG CUI

Key Laboratory of Cloud-Precipitation Physics and Severe Storms, Institute of Atmospheric Physics, Chinese Academy of Sciences, and University of Chinese Academy of Sciences, Beijing, and Collaborative Innovation Center on Forecast and Evaluation of Meteorological Disasters, Nanjing University of Information Science and Technology, Nanjing, China

DA-LIN ZHANG

Department of Atmospheric and Oceanic Science, University of Maryland, College Park, College Park, Maryland, and Key State Laboratory for Severe Weather, Chinese Academy of Meteorological Sciences, China Meteorological Administration, Beijing, China

DONGXIA LIU

Key Laboratory of Middle Atmosphere and Global Environment Observation, Institute of Atmospheric Physics, Chinese Academy of Sciences, Beijing, China

DONG ZHENG

Key State Laboratory for Severe Weather, Chinese Academy of Meteorological Sciences, China Meteorological Administration, Beijing, China

ABSTRACT

In this study, the spatiotemporal characteristics of cloud-to-ground (CG) and intracloud (IC) lightning flashes observed by Surveillance et Alerte Foudre par Interférometrie Radioélectrique (SAFIR)-3000 over the Beijing metropolitan region (BMR) during 2005–07 were investigated. The results showed the presence of 299 lightning days with 241 688 flashes, most of which were IC lightning flashes. Only 19% of the total flashes were CG lightning flashes; 14% of these CG flashes were positive. Most lightning activity occurred during the summer months (June–August), with a major diurnal peak around 1900 Beijing standard time (BST) and a secondary peak around 2300 BST. Spatial variations in flash density and lightning days both exhibited an obvious southeastwardly increasing pattern, with higher flash densities or more lightning days occurring in the southeastern plains and lower values distributed on the northwestern mountains. The Z ratio (IC/CG lightning flashes) exhibited a similar spatial pattern, but the percentage of positive CG lightning flashes showed an almost opposite pattern. The results also showed significant topographic effects on the spatiotemporal variations in lightning activity. That is, flash counts on the northeastern and southwestern mountains peaked in the afternoon, whereas those on the southeastern plains peaked in the late night to early morning, which could be attributed to the propagation of thunderstorms from the mountains to the plains. The results showed that the SAFIR-3000 lightning data are more useful than CG lightning data alone for forecasting the development and propagation of thunderstorms over the BMR.

Corresponding author e-mail: Xiaopeng Cui, xpcui@mail.iap.ac.cn

1. Introduction

Lightning is a natural electric discharge phenomenon consisting of cloud-to-ground (CG) and intracloud (IC) flashes, and accounts for many human casualties and tremendous property damage worldwide every year (Zhang et al. 2011). Lightning activity is closely associated with severe convective events that can exert significant impacts on human society and environments. Thus, much attention has been paid to the relationship between lightning activity and severe convective events. For example, MacGorman et al. (1989) studied two tornadic storms and found that IC flashes are typically governed by cloud particle interactions at heights of 7–9 km and cyclonic shears at lower altitudes, whereas CG flashes are primarily determined by the distances between positive and negative charge centers. Williams et al. (1989) attributed IC flashes to the accumulation of graupel particles in the central dipole region, and the subsequent CG lightning activity to decreased ice particles below the main negative charge region. MacGorman and Burgess (1994) examined the relationship between CG flashes and severe convective events in 15 thunderstorms with large hailstones and tornadoes. They showed that large hailstones were observed when positive CG flashes dominated, whereas tornadoes frequently occurred during or after the positive CG flashes peaked, suggesting that positive CG flashes are frequently related to severe thunderstorms. Carey and Rutledge (1998) found an extremely high Z ratio (i.e., IC/CG flashes) and the occurrence of predominantly positive CG lightning after a hailstorm became severe. Wiens et al. (2005) showed that although IC flashes account for more than 95% of total flashes, frequent positive CG flashes coincide with rapid increases in storm updrafts and hail production.

With the rapid growth of lightning detection networks worldwide during the past few decades, observational data over long time periods have become available for studying the statistical nature and climatology of lightning and convective activity. Spatiotemporal distributions, polarity, flash multiplicity (i.e., number of return stokes in a lightning flash), and peak current have been analyzed, mainly based on CG flash data, to reveal various lightning characteristics in different geographical regions (Takeuti et al. 1978; Schulz et al. 2005; Rivas Soriano et al. 2005; Burrows and Kochtubajda 2010; Villarini and Smith 2013; Poelman 2014; Xia et al. 2015). Statistical analyses have also been conducted on the relationship between lightning activity and topographic influences. Kotroni and Lagouvardos (2008) analyzed 1-yr CG lightning data in the Mediterranean Sea region and found that the relationship between

lightning and terrain elevation differs from season to season. Bourscheidt et al. (2009) analyzed CG lightning density in south Brazil, and indicated that it is better correlated with terrain slope rather than elevation. Vogt and Hodanish (2014) studied 10-yr CG lightning data in Colorado and revealed a positive correlation between lightning activity and terrain elevations lower than 1829 m (6000 ft) or above 3200 m (10 500 ft). Cummins (2014) indicated that topography not only affects the incidences and locations of lightning activity but also influences the physical parameters of CG flashes.

With the recent development of advanced lightning detection networks capable of observing IC flashes, some IC flash-related statistical studies have been carried out. By using 4-yr observations of CG and IC lightning data in the continental United States, Boccippio et al. (2001) found that the Z ratio is correlated with ground elevation, but little evidence to support a latitudinal correlation. They also found that local high Z ratio anomalies coincide with anomalies in the percentage of positive CG flashes relative to the total CG flashes (P_{PCG}). By examining the climatology of IC lightning characteristics, Pinto et al. (2003) found that P_{PCG} is correlated with IC flashes in the north of Brazil. Similar results were found by Rivas Soriano and de Pablo (2007). More recent studies have indicated that total lightning (CG and IC) data are more useful than CG lightning data alone for severe-weather warnings (Schultz et al. 2011; Chronis et al. 2015; Nishihashi et al. 2015). Therefore, statistical analyses of lightning characteristics using both CG and IC lightning data should provide a better understanding of the statistical nature and climatology of lightning activity and the associated severe convective weathers, which has not been studied in depth until now.

Numerous studies have examined the lightning characteristics over the Beijing metropolitan region (BMR) and its adjacent regions, mainly based on CG lightning data. These studies have shown that more lightning activity occurs during the summer months (June–August), with the main peak in the afternoon and a secondary peak at night, and more lightning activity occurring over its southwestern and northeastern mountains (Qie et al. 1991; He and Li 2005; Zheng et al. 2005; Zhou et al. 2009; R. Li et al. 2013). As previous studies have not included IC flashes, which usually account for a large percentage of total lightning activity, their results only provide a limited understanding of lightning characteristics. In fact, Xue et al. (1999) used both CG and IC lightning data at a single station to examine the lightning activity in Beijing's summer season, but found a higher-than-expected percentage of CG flashes (i.e., 46%–79%). As the lightning location system they used only had a

low-frequency (i.e., 500–350 kHz) sensor with limited ability to detect IC lightning, their results appeared to underestimate the amount of IC flashes. J. Li et al. (2013) used the data from Surveillance et Alerte Foudre par Interférometrie Radioélectrique (SAFIR)-3000 to study the spatiotemporal variations in lightning activity over north China. They found that CG and IC flashes have similar characteristics, except that the IC flashes have one diurnal peak whereas CG flashes have two diurnal peaks. Their study was concentrated on north China, but the detailed CG and IC lightning characteristics over the BMR were not clearly revealed.

In this study, lightning data measured by the Beijing SAFIR-3000 lightning location system were used. The data have been successfully applied to analyze lightning activity in severe convective events over the BMR (Zheng et al. 2009; Liu et al. 2011, 2013). Zheng et al. (2009) studied the total lightning characteristics and electric structural evolution in a hailstorm and found that IC lightning discharges constitute the main part of the total lightning and that the average P_{PCG} of 20% is higher than that in a normal storm. Liu et al. (2011) studied the total lightning activity in a leading-line and trailing stratiform mesoscale convective system (MCS) over the BMR. They found that most lightning flashes are IC flashes with 25% mean positive CG flashes, and that most of the IC lightning occurs at an altitude of about 9.5 km. Later, Liu et al. (2013) deduced electric charge structures using this lightning data and revealed that the vertical structure of lightning radiation sources evolves from two layers into three layers in a squall line over north China. These case studies showed that the SAFIR-3000 lightning data are very useful for gaining a better understanding of lightning characteristics. The major purpose of the present study was to determine what new lightning characteristics over the BMR could be found by analyzing both CG and IC flashes during the 3-yr period of 2005–07. In particular, we aimed to gain some new knowledge on the relationship between lightning activity and topography over the BMR, with the overarching goal of showing the utility of the SAFIR-3000 data for improving convective weather forecasts.

The next section describes the data and methodology used in this study. Section 3 presents a statistical analysis of the CG and IC lightning flashes, including annual, monthly, diurnal, and spatial variations. A summary and concluding remarks are given in the final section.

2. Data and methodology

The BMR is the capital of China and occupies an area of 16 410 km^2, with a population of about 21.7 million
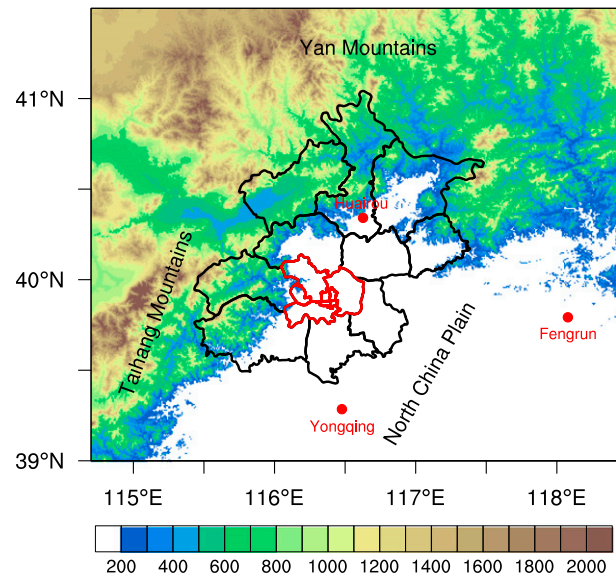

FIG. 1. Locations of the three SAFIR-3000 substations (red dots) and topography over the BMR and its adjacent areas (shaded; m). The black line denotes the BMR, and the red line denotes its urban area.

(Beijing Municipal Bureau of Statistics 2015). Before studying the lightning characteristics over the BMR, it is necessary to first describe its topography. As shown in Fig. 1, the BMR is surrounded by the Yan Mountains in the north and the Taihang Mountains in the west (1000–1500 m) and is open to the north China plains in the southeast (20–60 m). Sharp terrain slopes between the mountains and the plains occur over the BMR. The convective activities are closely related to the topography. Previous studies have indicated that deep convective activities are often triggered over foothills (Wang et al. 2014) and then propagate from the mountains to the plains (Chen et al. 2011). Observations have also shown that thunderstorms usually experience rapid intensification over foothills and intensify further after moving over the plains (Chen et al. 2011; Huang et al. 2012). Furthermore, recent lightning studies have shown that rapid increases in total lightning flashes are well correlated with intensifying thunderstorms (Chronis et al. 2015; Schultz et al. 2015).

Lightning data used in this study were obtained from the SAFIR-3000 lightning location system, which is a three-dimensional multistation detection system that can discriminate between CG and IC flashes. Each station in the system has a very high frequency (VHF) sensor (110–118 MHz) and a low-frequency (LF) sensor (300 Hz–3 MHz). The VHF sensor provides accurate angular localization of IC flashes, and the LF sensor mainly detects CG flashes. The SAFIR-3000 sensors detect the time, location, polarity, and peak current of
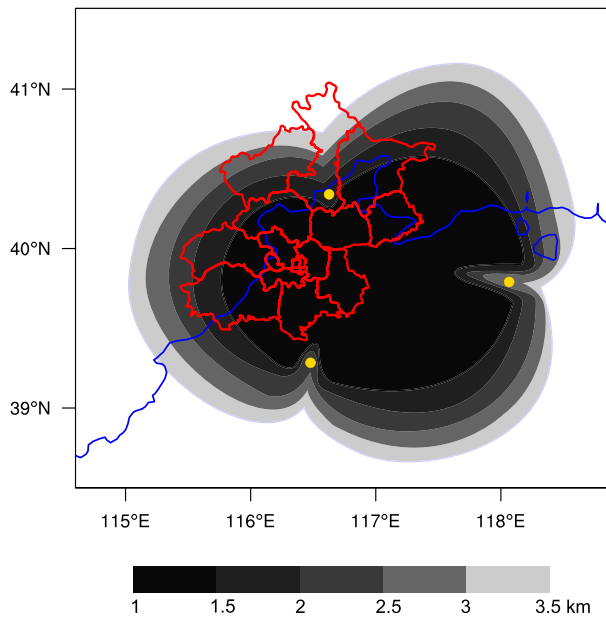
FIG. 2. Spatial distribution of location accuracy of the Beijing SAFIR-3000 lightning detection network. The gray shades give the localization errors (km), and the yellow points mark the three substations. The blue lines denote the 200-m terrain elevation. (The figure is redrawn from a picture provided by Vaisala.)
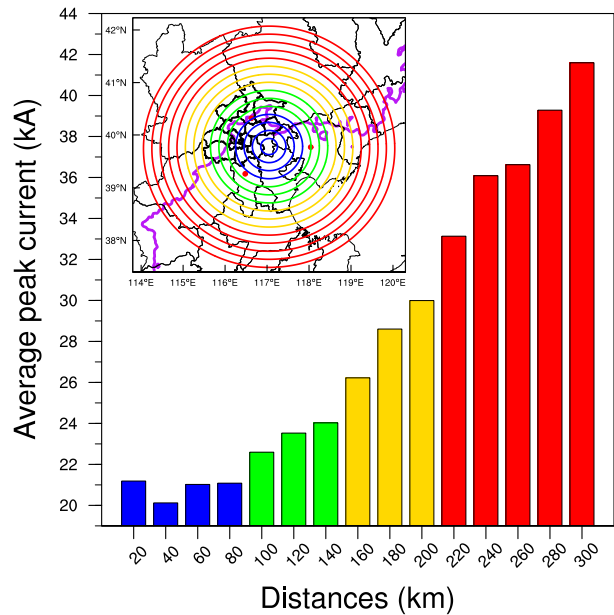

FIG. 3. Distance variations in the mean peak current (kA). Data are computed from the negative CG flashes in the SAFIR-3000 dataset during 2005–07 and are averaged over concentric rings from the center of the three substations with radii at 20-km intervals (inset). Blue, green, yellow, and red bars and concentric rings denote the distance ranges of 0–80, 80–140, 140–200, and 200–300 km, respectively. Purple lines in the insert denote the 200-m terrain elevation.

the radiation sources associated with lightning. The Beijing SAFIR-3000 lightning detection network consists of the following three substations (Fig. 1): Huairou District of Beijing (40°21′N, 116°37′E), Yongqing (39°18′N, 116°28′E), and Fengrun (39°47′N, 118°5′E) of Hebei Province. The distance between each substation is about 120 km, and the detection area covers 270–280 km^2 of the BMR and its surroundings. The locations of radiation sources are detected using the method of triangulation through GPS time-synchronized direction of arrival provided by interferometric sensors at the three substations and then transmitted to the central station at the Beijing Meteorological Bureau.

It is claimed that both the LF and VHF sensors of SAFIR-3000 have a detection efficiency of up to 90% and a location error of less than 2 km in an effective detection area of around 200 km from the center of the substations (Zheng et al. 2009). However, evaluations of SAFIR-3000 in other places have found that the lightning detection network may not achieve the claimed performance (Gao 2009); thus, the spatial variations in location accuracy and detection efficiency should be discussed carefully first. The spatial variation in the location accuracy shows that the best detection area is inside the triangle defined by the three substations, and location errors increase significantly with increasing distance from the center of the triangle (Fig. 2). The area

with a location error of less than 2 km covers most of the BMR, including the southeastern plains (less than 1.5 km), the southwestern mountains, and the northeastern mountains. The lowest location accuracies occur over the northwestern mountains (2.0–3.5 km), especially in the northern margins of the BMR (greater than 3.5 km). Unfortunately, the spatial variation in detection efficiency is not provided by Vaisala, Inc., the supplier of SAFIR-3000. However, it can be reflected in the spatial variation of lightning peak current, because fewer lightning flashes with a lower peak current should be observed with decreasing detection efficiency (Gao 2009). As mentioned above, it can be seen that the mean peak current significantly increased with distance from the center of the SAFIR-3000 network (Fig. 3). From the distance variations in mean peak current, it can be inferred that the best detection efficiency is within the triangle of the three substations (with a distance range of 0–80 km), because the values of mean peak current remained at a low level with little variation (blue colors in Fig. 3). Obvious decreases in the detection efficiency were divided into three distance ranges (green, yellow, and red colors in Fig. 3). In the BMR, the SAFIR-3000 network had the best detection efficiency over the southeastern plains, and had some decreasing detection

TABLE 1. Lightning statistical characteristics over the BMR during 2005–07.

Year	Total	IC	CG	PCG	NCG	CG/total (%)	Positive CG/CG (%)	Z ratio (IC/CG)
2005	49 659	33 282	16 377	1825	14 552	32.98	11.14	2.03
2006	109 117	94 062	15 055	2509	12 546	13.80	16.67	6.25
2007	82 892	69 445	13 447	1724	11 723	16.22	12.82	5.16
2005–07	241 668	196 789	44 879	6058	38 821	18.57	13.50	4.38

efficiency in the southwestern and northwestern mountains. The network performed poorly in the western and northern margins of the BMR. The decrease in detection efficiency was more significant for the VHF sensors (IC flashes) than the LF sensors (CG flashes) and more significant for the negative CG flashes than the positive. Therefore, the nonhomogeneous spatial variations in the detection efficiency and location accuracy over the BMR should be considered when the spatial variations in lightning characteristics are discussed. The SAFIR-3000 lightning detection network began a test run in 2003, and the substations and central station were updated and maintained twice in 2003 and 2004. From 2005, the network maintained stable operations until one of the sensors broke down in 2008. The lightning data (both CG and IC) during the 3-yr period of 2005–07 are believed to be optimal because of the best performance of the network in this period. Therefore, in this study, the lightning statistics over the BMR were examined by using the 3-yr (2005–07) SAFIR-3000 lightning data.

The SAFIR-3000 lightning location system only detects radiation sources associated with IC flashes, but one IC flash usually produces one or more radiation sources. Thus, data quality control was necessary to group radiation sources into lightning flashes, following Liu et al. (2011). In this method, radiation sources detected within 1 s and at a distance of less than 10 km from each other are grouped together as a lightning flash. And the arrival time, position, altitude, etc. of the first recorded radiation source are regard as the attributes of the lightning flash. Since previous IC observations in north China have shown little IC lightning activity occurring below 1 km, IC flashes below 1 km in this lightning network were removed. Furthermore, previous radar observations have shown that cloud tops over the BMR seldom exceed 16-km altitude, so IC flashes at altitudes higher than 18 km were considered unrealistic and were also neglected. Similarly, the first return stoke is treated as a CG flash in SAFIR-3000. As in previous studies (Antonescu and Burcea 2010; Poelman 2014; Taszarek et al. 2015), a positive CG flash with a peak current of less than 10 kA was considered as an IC flash.

CG flash density (i.e., the number of flashes per square kilometer) is usually computed on 10 km × 10 km (or

0.1° × 0.1°, longitude × latitude) or 20 km × 20 km (or 0.2° × 0.2°, longitude × latitude) grid cells (Antonescu and Burcea 2010; Liou and Kar 2010; Taszarek et al. 2015; Xia et al. 2015). In this study, 0.1° × 0.1° (longitude × latitude) grid cells were used to compute the CG flash density. The same computation method was also applied to the IC flash density, P_{PCG}, and Z ratio. A lightning day in the BMR was defined as a day with at least two observations of lightning flashes (CG or IC) in area of the BMR. To examine the spatial variation in lightning days, the grids with a resolution of 0.01° × 0.01° (longitude × latitude) are used to provide smoother climatology maps of lightning days. And the lightning day on the grids was defined as a day with at least two observations of lightning flashes (CG or IC) in a range of 15 km around the grids. Similar methods have been used by Czernecki et al. (2016), Enno (2015), Novák and Kyznarová (2011), and Taszarek et al. (2015), as the combination of threshold values has proven to provide lightning days that best correspond to human observations. The lightning days data were divided into five intensity grades according to their daily flash counts (2–10, 11–100, 101–1000, 1001–10 000, and >10 000), following Taszarek et al. (2015), to determine the intensity of the thunderstorms contributing to the BMR's lightning statistics.

3. Results

a. Annual variations

The 3-yr lightning statistics showed the occurrence of 196 789 IC flashes and 44 879 CG flashes over the BMR, with large year-to-year variability (Table 1). Clearly, most of the lightning flashes were IC flashes (81.4%), and CG flashes only accounted for a small portion of the total flashes (18.6%); 13.5% of these CG flashes were positive. The Z ratio has been used to understand the characteristics of IC flashes in relation to latitude and altitude (Price and Rind 1993; Boccippio et al. 2001). The BMR's 3-yr and regionally averaged Z ratio was 4.38 as compared with a zonally averaged Z of 2.64–2.94 over the continental United States (latitude: 25°–50°N; altitude: 0.5–1.7 km) (Boccippio et al. 2001) and 3.48 over the Iberian Peninsula (latitude: 35°–44°N) (Rivas

TABLE 2. Intensity grade distributions of total lightning days (2005–07), lightning days per year, and their percentages relative to those summed for all intensity grades over the BMR. As with lightning days, the intensity grade distributions of total flash counts are also displayed.

Intensity grade	Grade definition	No. of days (2005–07)	No. of days per year	Percentage (%)	Total flash counts (2005–07)	Total flash counts per year	Percentage (%)
1	2–10	124	41	41.47	392	131	0.16
2	11–100	53	18	17.73	2136	712	0.88
3	101–1000	67	22	22.41	28 834	9611	11.94
4	1001–10 000	52	17	17.39	168 660	56 220	69.84
5	>10 000	3	1	1.00	41 471	13 824	17.18
	All	299	99	100.00	241 493	80 498	100

Soriano and de Pablo 2007). This implies that IC flashes are more common in the BMR than in the above regions. In particular, Table 1 shows that the annual IC flash rate varied by nearly a factor of 3. All this indicates that a spatiotemporal analysis of both IC and CG flashes, as described in the next three subsections, is highly desirable for understanding lightning characteristics over the BMR.

During the 3-yr period of 2005–07, a total of 299 lightning days (about 99 days yr^{-1}) were identified over the BMR, which produced a total of 241 493 lightning flashes. To estimate the intensity of lightning days, the flashes were divided into five intensity grades (1–5) with daily total flash counts of 2–10 (124 days), 11–100 (53 days), 101–1000 (67 days), 1001–10 000 (52 days), and >10 000 (3 days). It is evident from Tables 2 and 3 that the grade 4 lightning days were the most influential lightning events during the study period, because they produced 70% of the total flashes and had the most lightning hours. Lightning days in grades 1 and 2 accounted for more than half of the total lightning days (177 days), but they only made a small contribution to the total number of lightning flashes (about 1%). Thus, their characteristics were hard to see when all grades were considered together. In contrast, although there were only three cases of the most intense lightning days (grade 5) during the study period, they produced a large number of lightning flashes (Table 4); thus, they should not be neglected. Therefore, it was necessary to divide

lightning days into different intensity grades and discuss the lightning characteristics at different intensities. Table 3 shows the durations and lightning-producing efficiencies of the lightning days. An evaluation of the average duration hours per lightning day revealed that lightning hours increased with lightning intensity (e.g., from 1.8 h in grade 1 to 9.8 h in grade 4) but remained nearly constant when reaching grades 4 and 5. Similarly, the flash counts per lightning day and per lightning hour both showed rapid increases with intensity grades, much faster than the increased duration hours. This implies that lightning-producing efficiency (i.e., flashes per lightning day or lightning hour) was a more significant characteristic than duration during intense lightning days. A further analysis of the lightning properties, given in Table 5, showed that the more intense the lightning days were, the more frequent IC flashes were [as exhibited by the percentage of CG flashes (P_{CG}) and the Z ratio, except for grade 1], and the less frequent positive CG flashes were (as shown by P_{PCG}).

b. Monthly variations

The monthly variations in both CG and IC flash counts showed a well-defined thunderstorm season during the summer months from June to August, with 94%–96% of the total flash counts in a year occurring in these months (Fig. 4). A much smaller number of flash counts were seen during the spring (March–May) and autumn (September–November) months, and there

TABLE 3. Intensity grade distributions of lightning hours (2005–07), lightning hours per lightning day, total flash counts per lightning day, and total flash counts per lightning hour over the BMR.

Intensity grade	Grade definition	No. of hours (2005–07)	Lightning hours per lightning day	Flash counts per day	Flash counts per hour
1	2–10	225	1.8	3.2	1.7
2	11–100	197	3.7	40.3	10.8
3	101–1000	475	7.1	430.4	60.7
4	1001–10 000	511	9.8	3243.5	330.1
5	>10 000	30	10.0	13 823.7	1382.4
	Total	1438	4.8	807.7	167.9

TABLE 4. Lightning statistical characteristics of the three most intensive lightning days during 2005–07.

Lightning day	Date	Total	CG	IC	P_{PCG} (%)	Z	Peak hour (BST)
1	31 Jul 2006	16 324	726	15 598	33.06	21.5	1000
2	1 Aug 2007	14 498	2431	8218	5.68	3.4	2200
3	17 Jul 2007	10 649	1772	12 726	10.78	7.2	0700

were almost none during the winter months (December–February). The monthly peak lightning activity during the summer months has also been found in the CG lightning statistics over the BMR (He and Li 2005; J. Li et al. 2013; R. Li et al. 2013) and elsewhere, such as Romania (Antonescu and Burcea 2010), Belgium (Poelman 2014), and Poland (Taszarek et al. 2015). This peak lightning activity is mainly attributed to the monsoon-related regional climate, with rich, warm, and humid air transported to the BMR during the summer months, which favors the presence of thermodynamic instability for convective activity (J. Li et al. 2013; Wang et al. 2014). Like the CG flashes, IC flashes were also concentrated during the summer months. However, the peak IC flash counts occurred in July, whereas the peak CG flash count was in August. This suggests that taking IC flashes into consideration is necessary for depicting the monthly variation in total lightning flashes. It can also be seen that the percentage of CG flashes (P_{CG}) varied from 10% in spring and autumn to a peak value of 28% in August (Fig. 4). Of interest is that while the CG flash counts increased during the summer months, P_{PCG} displayed an almost opposite trend with a minimal value in August. One explanation for the high P_{PCG} in the colder seasons is that the upper positively charged air is often advected away from the lower negatively charged air, because of the presence of large vertical wind shear, and therefore exposed to the ground directly (Takeuti et al. 1978; Brook et al. 1982; Engholm et al. 1990). Predominant positive CG flashes are often observed in shallow clouds of MCSs (Engholm et al. 1990; Qie et al. 2002), while negative flashes tend to occur in deep convective regions (Rakov and Uman 2003, 214–234). As thunderstorms during colder seasons are usually accompanied with shallower convection, they are more likely to produce positive flashes than those in summer.

The monthly distribution of the 3-yr-averaged lightning days showed a single peak (about 19 days yr^{-1}) in July and over half of the lightning days (54 days yr^{-1}) occurred during the summer months (Fig. 5). The spring and autumn months had similar lightning days (22 and 17 days yr^{-1}, respectively) and the fewest seasonal lightning days (5 days yr^{-1}) occurred during the winter months. The 3-yr-averaged lightning hours (i.e., at least one flash per hour) showed that the most frequent lightning activity occurred during the summer months, ranging from 300 to 400 h month^{-1}, as compared with fewer than 100 h month^{-1} in the other seasons (Fig. 5). The 3-yr-averaged lightning hours per day declined from 7.3 to 6.0 h day^{-1} from June to August (Fig. 5), indicating that on average the duration of lightning hours in June lasted 1.3 h longer than those in August. The results revealed that lightning days in August were more intense than those in June because they had more lightning flashes within shorter durations.

Figure 6 shows the monthly variation of the percentages of the five intensity grades. The results showed that grade 1 lightning days were dominant in the cold season when thunderstorms were inactive (Fig. 4). After entering the warm season (May–September), grade 1 lightning days dropped rapidly to less than 10% in June. At the same time, more intense lightning days increased rapidly, and grade 3 and 4 lightning days increased to 40% and 29% in June, respectively. The summer months were dominated by grade 4 and 5 lightning days and accounted for 38% of the total lightning days at their peaks in July. It is evident from the monthly variation of CG and IC flash counts in the different intensity

TABLE 5. Intensity grade distributions of the total, IC, CG, PCG, and NCG flashes, and the percentage of CG flashes relative to total flashes (P_{CG}), the percentage of positive CG flashes relative to CG flashes (P_{PCG}), and Z ratio during the 3-yr period of 2005–07 over the BMR.

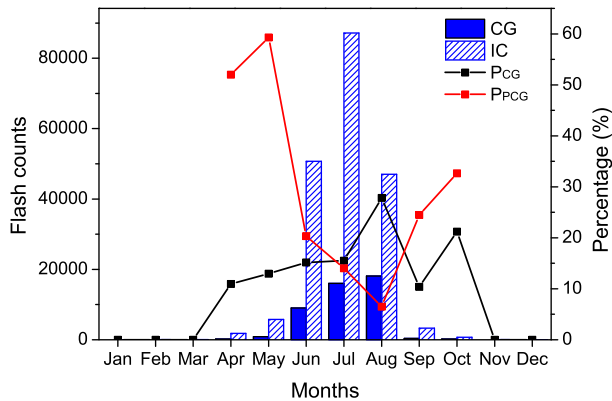| Intensity grade	Grade definition	Total	IC	CG	PCG	NCG	P_{CG}	P_{PCG}	Z
1	2–10	392	362	30	9	21	7.65	30.00	12.07
2	11–100	2136	1583	553	167	386	25.89	30.20	2.86
3	101–1000	28 834	22 896	5938	1248	4690	20.59	21.02	3.86
4	1001–10 000	168 660	135 263	33 397	4046	29 351	19.80	12.11	4.05
5	>10 000	41 471	36 542	4929	569	4360	11.89	11.54	7.41
	Total	241 493	196 646	44 847	6039	38 808	18.57	13.47	4.38

FIG. 4. Monthly variations of CG (filled bars) and IC (hatched bars) flash counts, the percentage of CG flashes relative to total flashes (P_{CG}; black), and the percentage of positive CG flashes relative to the CG flashes (P_{PCG}; red), which are derived from the SAFIR-3000 data for the 3-yr period of 2005–07 over the BMR.
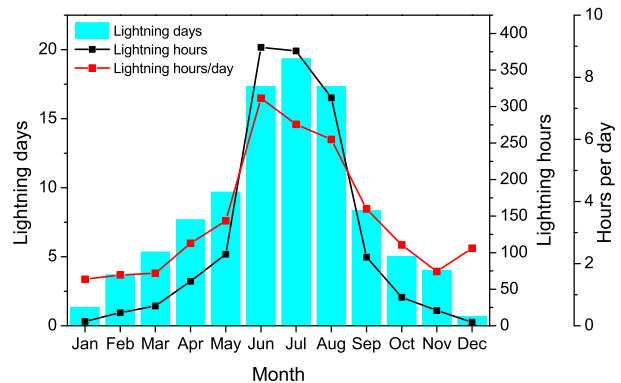

FIG. 5. Monthly variations in lightning days (bars), lightning hours (black), and lightning hours per lightning day (red). All data are computed for the 3-yr period of 2005–07 over the BMR.

grades that both CG and IC flash counts in almost all grades mainly occurred during the summer months (Fig. 7), except for the IC flash counts in grade 1 with more flashes during the spring and autumn months.

c. Diurnal variations

Previous lightning statistics have shown that the diurnal variation in CG lightning activity over the BMR usually exhibits a bimodal shape with two peaks, one in the late afternoon and the other at night, with a minimum in the late morning (He and Li 2005; Zheng et al. 2005; Zhou et al. 2009; J. Li et al. 2013). Similar to previous studies, both CG and IC flash densities displayed a main peak around 1900 BST and a secondary peak around 2300 BST (Fig. 8a). However, we could see active lightning occurring during the morning hours, with a peak of CG (IC) lightning around 0600 BST (1000 BST), which has not been mentioned in previous lightning statistics. However, the pronounced lightning activity coincided well with a separate rainfall peak usually found in the early morning after some MCSs propagated from the western mountains to the southeastern plains (Li et al. 2008; Yin et al. 2011; Yang et al. 2013; Yuan et al. 2014).

Some previous studies have shown the influence of the mountain–plain circulation on the diurnal variations in convective initiation and precipitation over the BMR (Yin et al. 2011; Yuan et al. 2014). Such topographical influences can be clearly seen in Fig. 9. The peak flash counts in the northeastern and southwestern mountainous areas mainly occurred in the afternoon, while those in the southeastern plains often occurred at night or in the morning. The results are consistent with the diurnal variation of precipitation that often initiates in

the afternoon over the mountainous regions and then propagates southeastward to the plains at night or in the morning (Yin et al. 2011; Yang et al. 2013; Yuan et al. 2014). Moreover, the peak CG and IC flash counts in the southeastern plains occurring around 0600 and 1000 BST, respectively, could explain well the lightning peaks in the morning hours shown in Fig. 8a.

While Fig. 8a shows typical smooth diurnal cycles of CG and IC flashes, their corresponding percentages (i.e., P_{CG} and P_{PCG}) and Z ratio exhibited irregular fluctuations (Fig. 8b). Part of the fluctuations may be attributed to the development of a few intense thunderstorms with extreme lightning activity (Table 4). For example, an intense thunderstorm on 31 July 2006 produced 16 324 total flashes, with an extremely high Z ratio (21.5), over the BMR. This broke the daily flash rate record during the period of 2005–07 and caused a sharp rise in the Z ratio and a decline of P_{CG} around 1000 BST. Despite the presence of pronounced fluctuations, some evident
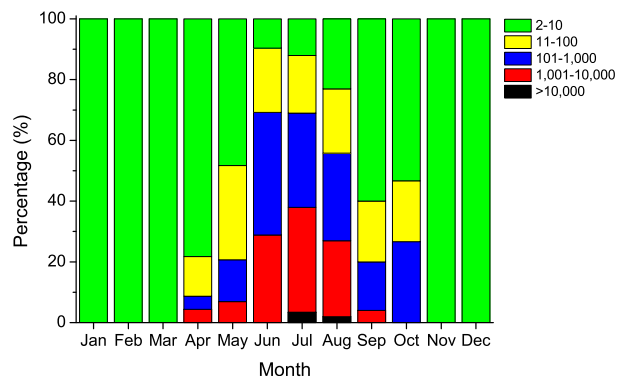

FIG. 6. Monthly variations in the percentages of the five different intensity grade lightning days relative to the total lightning days. All data are computed for the 3-yr period of 2005–07 over the BMR.
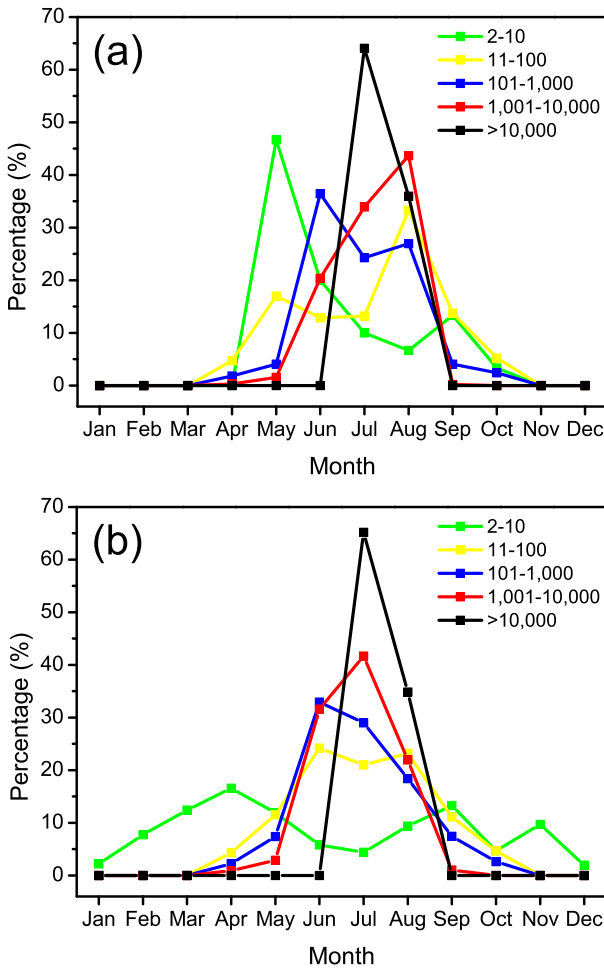
FIG. 7. Monthly variations in the percentages of (a) CG and (b) IC lightning flash counts relative to their annual amounts for the five different intensity grade lightning days.

FIG. 8. Diurnal variations of (a) CG (black) and IC (red) flash counts relative to their total daily amounts (%), and (b) P_{CG} (black), P_{PCG} (solid red), and Z ratio (dashed red). All data are computed for the 3-yr period of 2005–07 over the BMR.

characteristics could still be found from Fig. 8b. There was an obvious negative correlation (-0.83) between P_{CG} and P_{PCG}, indicating that P_{PCG} may be useful for estimating the percentage of CG or IC flashes when only CG lightning data are obtained. Furthermore, there was a positive correlation between the Z ratio and P_{PCG} (0.74) that roughly showed an increasing trend after 1200 BST and a declining tendency after sunset. This positive relationship has been reported elsewhere, such as the continental United States (Boccippio et al. 2001), northern Brazil (Pinto et al. 2003), and the Iberian Peninsula (Rivas Soriano and de Pablo 2007). This positive correlation could be helpful for severe-weather forecasters, as a high P_{PCG} value is often related to severe storms such as tornadoes and hailstorms (MacGorman and Burgess 1994).

More interesting information about the diurnal variations of lightning can be obtained when they are examined in the framework of the five intensity grades of
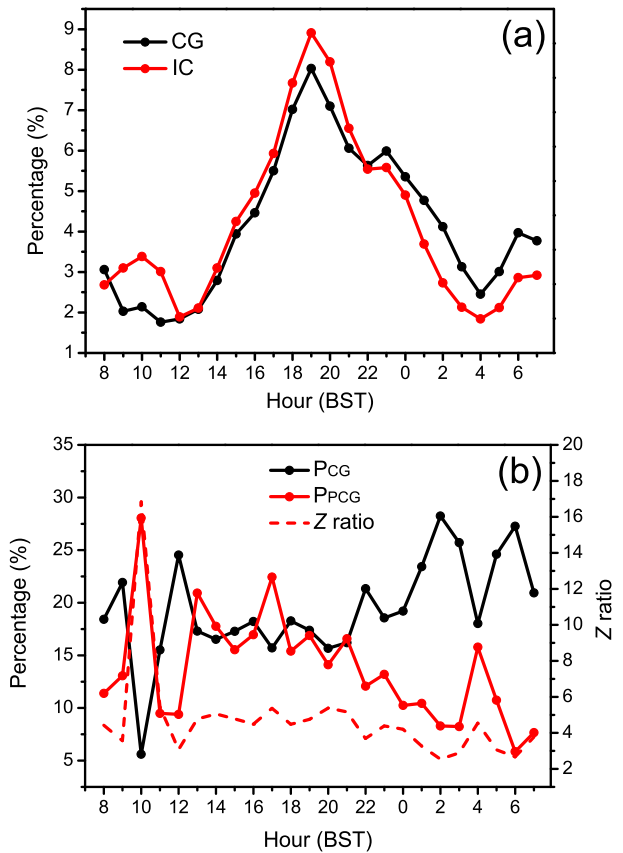
lightning days. We found five or six distinct diurnal peaks for the five intensity grades (Fig. 10). The main diurnal peaks for grades 1–4 occurred during 1600–1900 BST, with a tendency of more intense lightning days having their peak intensities occurring at later times, especially for the IC flashes. This tendency may be determined by the life span and organization of thunderstorms, as they were more active in later afternoon and tended to dissipate after sunset in the absence of larger-scale forcing. Both the CG and IC flashes had secondary diurnal peaks during 2300–0200 BST, which was consistent with the results shown in Fig. 8a. In comparison, grade 5 lightning days showed steep peaks in the morning hours, CG lightning at 0600 BST, and IC lightning at 1000 BST, with a secondary peak at 2200 BST (Table 4). The major peak accounted for the minor diurnal peak in the morning shown in Fig. 8a, and the secondary peak fitted well the above-mentioned tendency.

Spatial variations in the diurnal cycles of the different intensity grades are shown in Fig. 11, which shows more
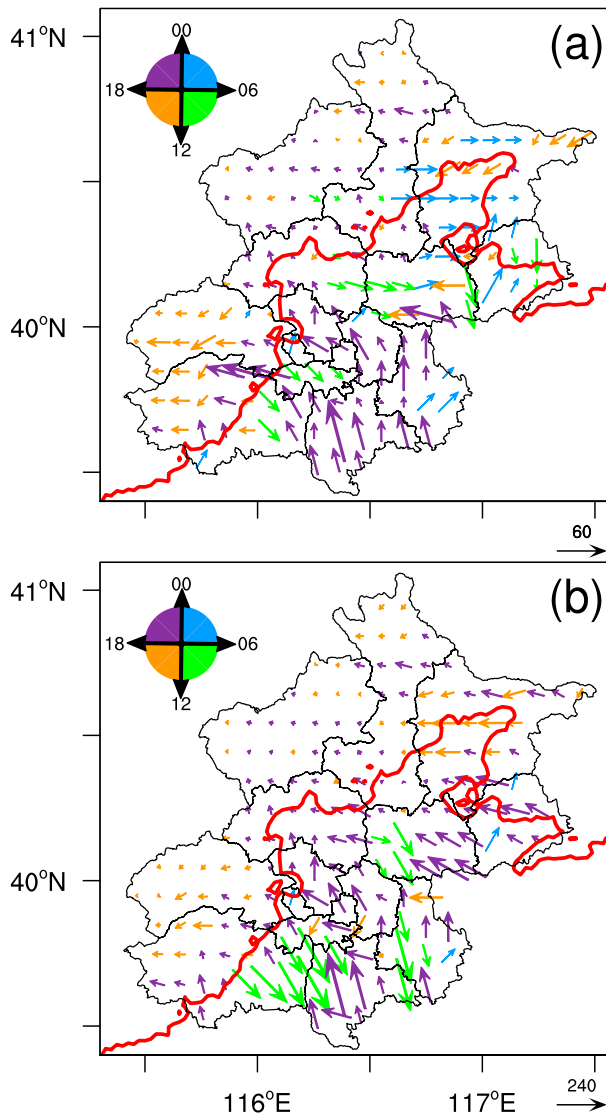
FIG. 9. Spatial distribution of the peak hourly (a) CG and (b) IC flash counts (flashes per hour) during the day on a 0.1° × 0.1° grid resolution for the 3-yr period of 2005–07 over the BMR. The vector length denotes peak hourly flash counts, and its direction denotes the corresponding peak hour (BST), which is illustrated by the clock in the top-left corner. The vector pointing north (east, south, west) indicates BST of 0000 (0600, 1200, 1800), and every 6-h interval shares a common color (e.g., 0100–0600 share the blue color). The red lines denote the 200-m terrain elevation.

organized structures of the peak flash vectors for higher-intensity grades. For example, grades 1 and 2 exhibited a few hourly flash counts in each grid, with the peak intensity occurring at all times (Figs. 11a,b). As the intensity grade increased, more organized flash vectors occurred in the afternoon over the southwestern mountains (Fig. 11c), and in the evening and early morning over the southeastern plains (Fig. 11d). The southeastward delayed diurnal phases were consistent
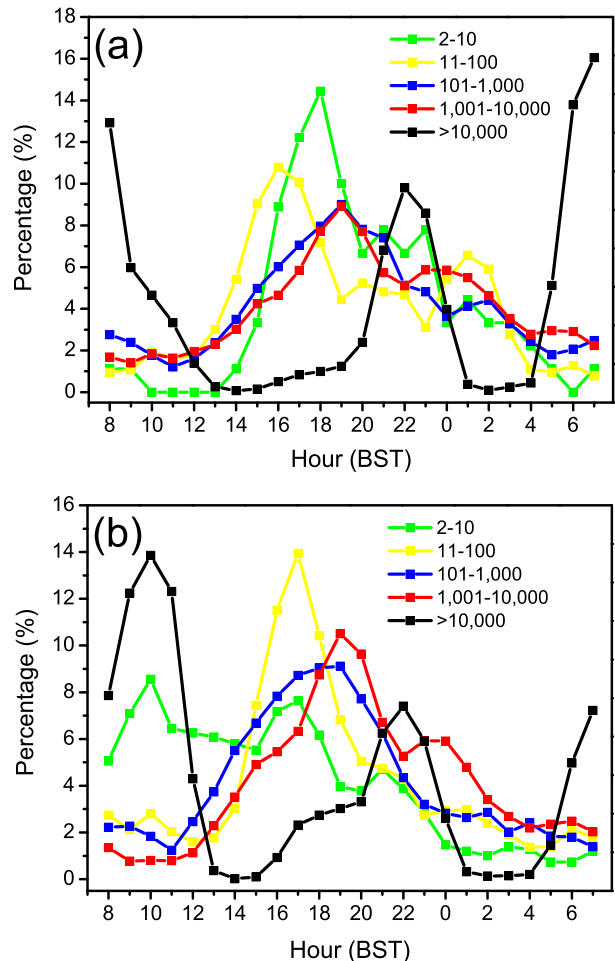

FIG. 10. Diurnal variations in the percentages of (a) CG and (b) IC lightning flash counts relative to their daily amounts for the five different intensity grade lightning days.

with those of precipitation and thunderstorm activity over the BMR, as revealed by previous studies (Chen et al. 2011; Yin et al. 2011; Wang et al. 2014; Yuan et al. 2014). Note that the organized peak flash vectors in the morning over the southeastern plains (Fig. 11e), as also indicated in Fig. 9, were mainly contributed by the three extremely strong lightning days in grade 5 (Table 4).

d. Spatial variations in flash density

It can be seen that the spatial variations in the flash density varied significantly from 2005 to 2007 (Fig. 12). Of significance is the contrast in flash density between the mountains and the plains, roughly separated by the 200-m terrain elevation. Despite the pronounced year-to-year variability in flash density, their spatial variation exhibited similar characteristics. Most flashes occurred in the southeastern plains (including the BMR's urban areas), and secondary large flash counts occurred over the foothills (i.e., around the 200-m elevation) in the
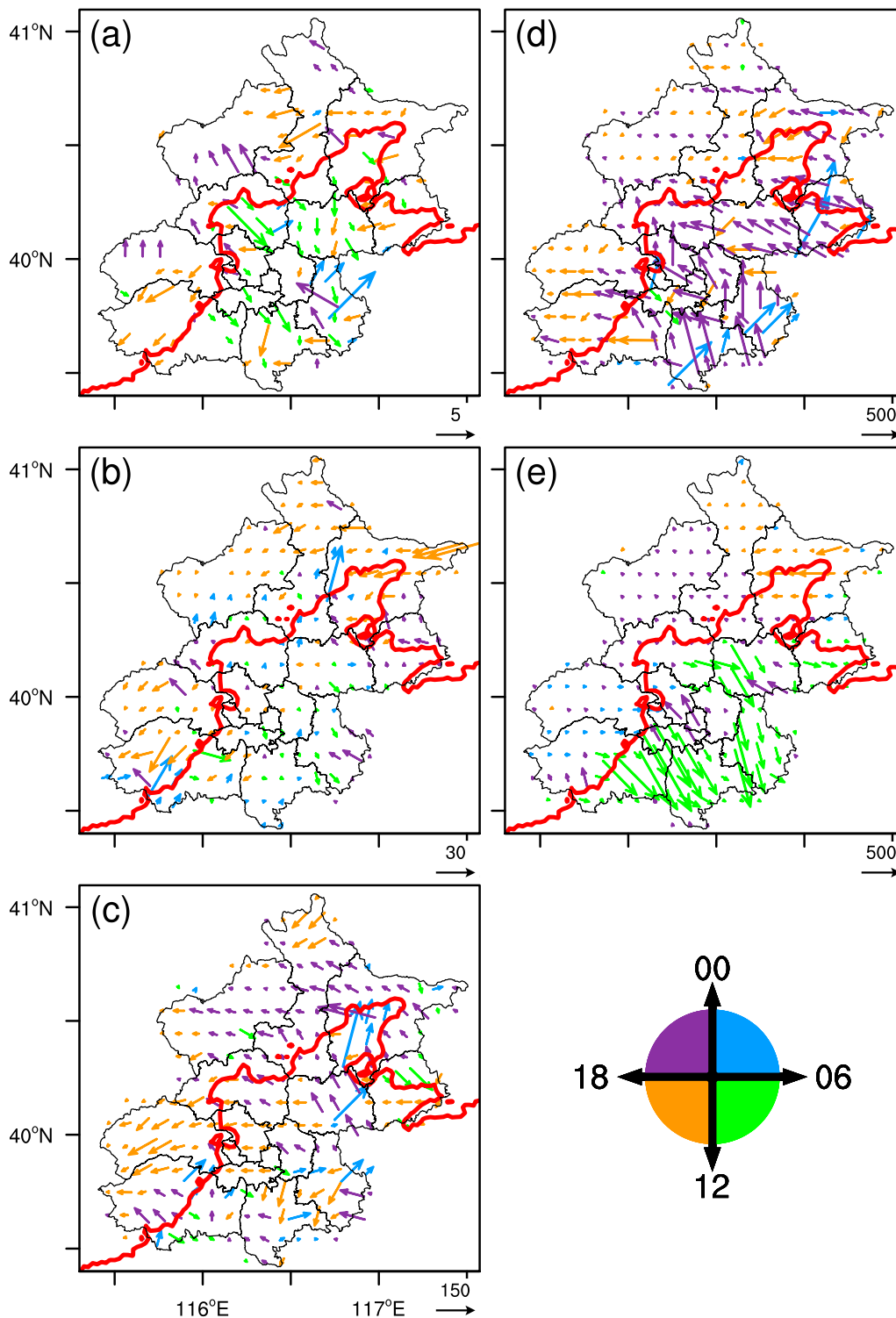
FIG. 11. Spatial distribution of the peak hourly total flash counts (flashes per hour) of the lightning days with intensity grades (a) 1, (b) 2, (c) 3, (d) 4, and (e) 5 on a 0.1° × 0.1° grid resolution during the 3-yr period of 2005–07 over the BMR. The vector length denotes peak hourly flash counts, and its direction denotes the corresponding peak hour (BST), as illustrated by the clock in the bottom-right corner. A vector pointing north (east, south, west) indicates BST of 0000 (0600, 1200, 1800), and every 6-h interval shares a common color.
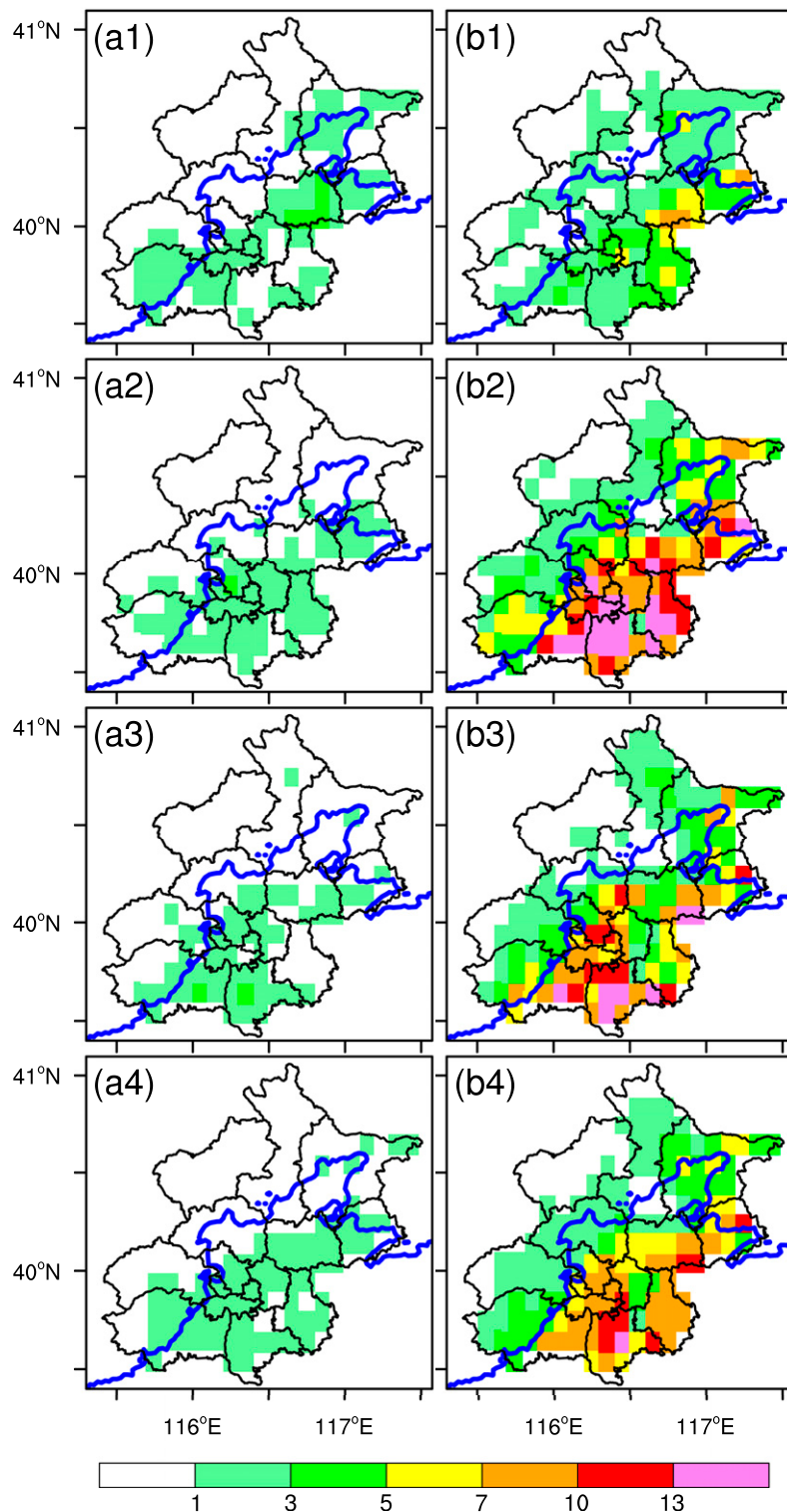
FIG. 12. Spatial distributions of flash density: shown are the CG flash densities for (a1) 2005, (a2) 2006, and (a3) 2007 (shaded; flashes per kilometer squared), along with (a4) the 3-yr means (shaded; flashes per kilometer squared per year); (b1)–(b4) as in (a1)–(a4), but for the IC flash density. The blue lines denote the 200-m terrain elevation.

northeastern and southwestern portions of the BMR. However, a much smaller number of flashes were observed in the northwestern mountainous regions, perhaps attributed to the deceasing detection efficiency in these regions. The results are consistent with previous CG lightning statistics that show lightning activity over the BMR is closely related to local topography and the underlying surface (He and Li 2005; Zheng et al. 2005; Zhou et al. 2009). Note that the above lightning statistics were mostly found in the IC flashes, and the CG flash densities were much smaller than IC flash densities. On average, the annual regional CG and IC flash densities were 0.91 and 3.95 flashes per kilometer squared per year, respectively, and exhibited similar southeastwardly increasing distribution patterns (cf. Figs. 12a,b). The annual CG flash density was slightly less than the 1.0–3.0 flashes per kilometer squared per year over the BMR obtained by R. Li et al. (2013) using CG lightning data from the advanced time of arrival and direction (ADTD) system. Evidently, the IC flash density complements our understanding of lightning activity and its relation to convective activity, because it dominates the total flash density (Fig. 12) and has more robust correlation with severe convective events (Schultz et al. 2011).

It can be seen that the spatial variations in the mean CG and IC flash densities during different seasons contrasted sharply (Fig. 13) (winter season is not shown because the values were too small). During the spring months, higher flash densities were found in the northeastern and southwestern mountainous areas for both CG (Fig. 13a) and IC flashes (Fig. 13d), implying that thunderstorms in spring usually initiate and dissipate over the mountainous regions and are short-lived. During the summer months, higher CG flash densities were found over the northeastern and southwestern foothills as well as the southeastern plains and urban areas, with maximum values of over 1.8 flashes per kilometer squared per year (Fig. 13b); higher IC flash densities were mainly found over the southeastern plains with maximum values of over 10.0 flashes per kilometer squared per year (Fig. 13e). Both the CG and IC flash densities showed the peak values in the plains, indicating the propagation of intensifying storms from the mountains to the plains with increased lightning flashes (Chen et al. 2011). A difference between them was that more CG flashes occurred over the urban area. This has also been found over the large urban areas of southeastern Brazil and attributed to possible thermal and aerosol effects (Naccarato et al. 2003). Flash density declined sharply from the summer months to the autumn months, with higher values (e.g., 0.05–0.10 CG flashes per kilometer squared per year and 0.30–1.00 IC flashes per kilometer squared per year) mainly occurring over the

northeastern and southwestern foothills (Figs. 13c,f). Unlike in the summer months, little lightning activity could be found over the BMR's urban areas.

e. Spatial variations in lightning days

The spatial variations in the lightning days are presented in Fig. 14. It can be seen that 2006 was the year of most frequent lightning days. Higher values were distributed on the northeastern and central foothills and in the southeastern plains (42–48 days), and in the southwestern mountainous areas (32–42 days) (Fig. 14b). On average (Fig. 14d), lightning days of at least 24 days yr^{-1} were observed in most parts of the BMR, and lightning days with higher values were located in the southeastern plains (about 40 days yr^{-1}) and on the foothills and mountains (about 30 days yr^{-1}). The northwestern mountains were the areas with the fewest lightning days. The impact of decreasing detection efficiency on the lightning day results was probably not as significant as the flash density, because only two flashes detected in a day can define a lightning day. Thus, the fewest lightning days observed on the northwestern mountains may be attributed to the weakest lightning activities. The spatial variations in lightning days also exhibited obvious monthly variations. Most of the lightning days occurred in the warm season (Figs. 15d–h), especially during the summer months (Figs. 15e–g). Higher values (over 10 days yr^{-1}) of lightning days were distributed in the mountainous areas in June (Fig. 15e) and in the southeastern plains in July (Fig. 15f), implying that thunderstorms in June tended to initiate and stay in the mountainous areas and those in July were more likely to propagate from the mountains to the plains. It is noteworthy that while flash counts in August were appreciable (Fig. 4), the lightning days (Fig. 15g) were obviously lower than those in June and July, with 6–8 days covering most parts of the BMR. This implies that thunderstorms in August were stronger and produced more flash counts in a lightning day than the other months, which confirms the results of Fig. 5.

The spatial variations in lightning days with different intensity grades showed that the most influential lightning days of grade 4 were widely distributed in the southeastern plains with a maximum of over 48 days (Fig. 16d), close to its 52 total lightning days, suggesting further the larger-scale influences of grade 4 lightning days. In contrast, although the weak lightning days of grade 1 had the most frequent occurrences of 124 days over the BMR, they were mainly distributed in the southeastern plains with a maximum of about 30 days, implying that weak lightning days influenced small regions and tended to be localized. The lightning days with moderate intensities (i.e., grades 2 and 3) were mostly
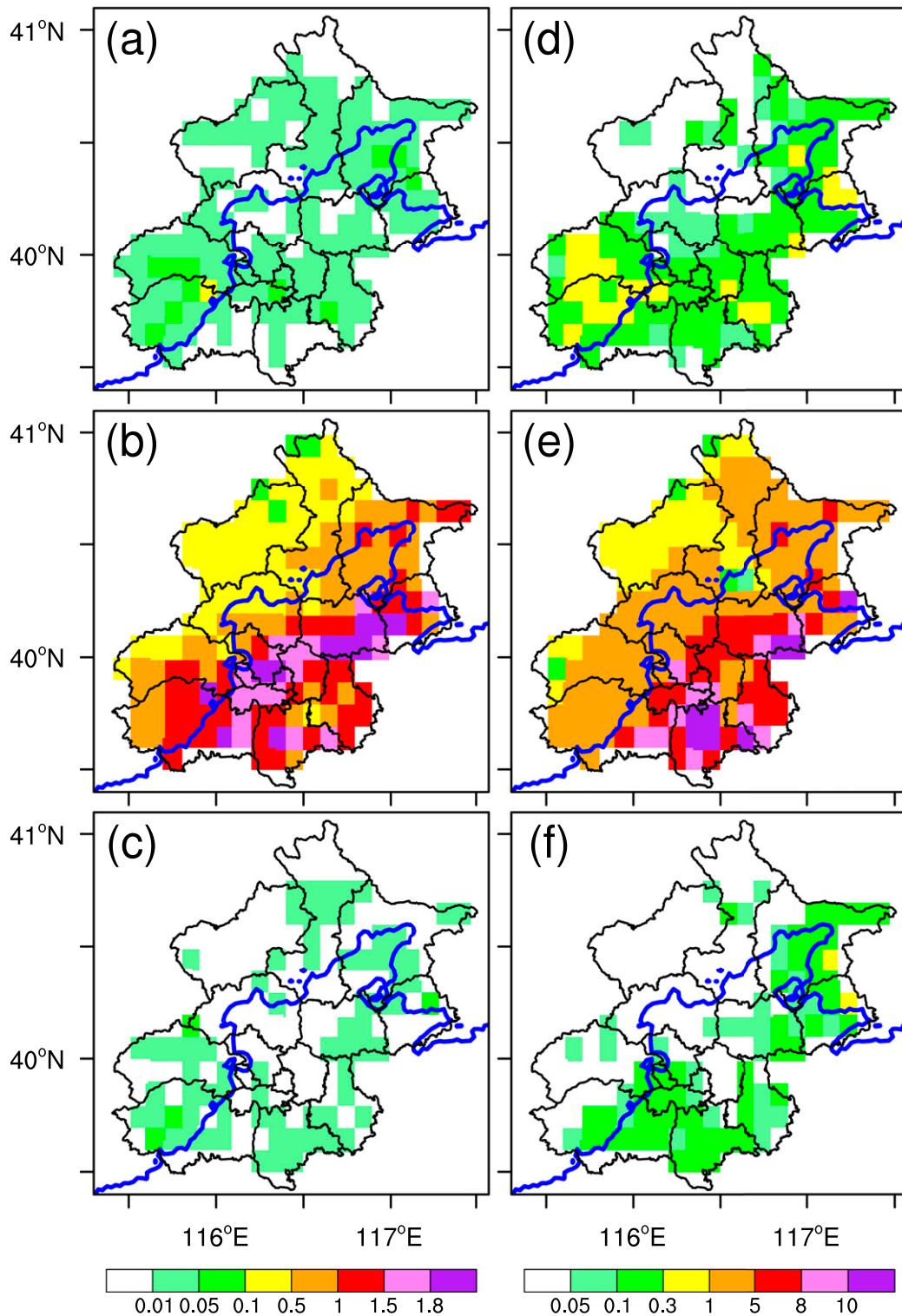
FIG. 13. Spatial distribution of the mean seasonal CG flash density (shaded; flashes per kilometer squared per year) for (a) spring (March–May), (b) summer (June–August), and (c) autumn (September–November) on a 0.1° × 0.1° grid resolution for the 3-yr period of 2005–07 over the BMR. (d)–(f) As in (a)–(c), but for IC flash density. The CG and IC flash densities during winter (December–February) are negligible and therefore are not shown. The blue lines denote the 200-m terrain elevation.
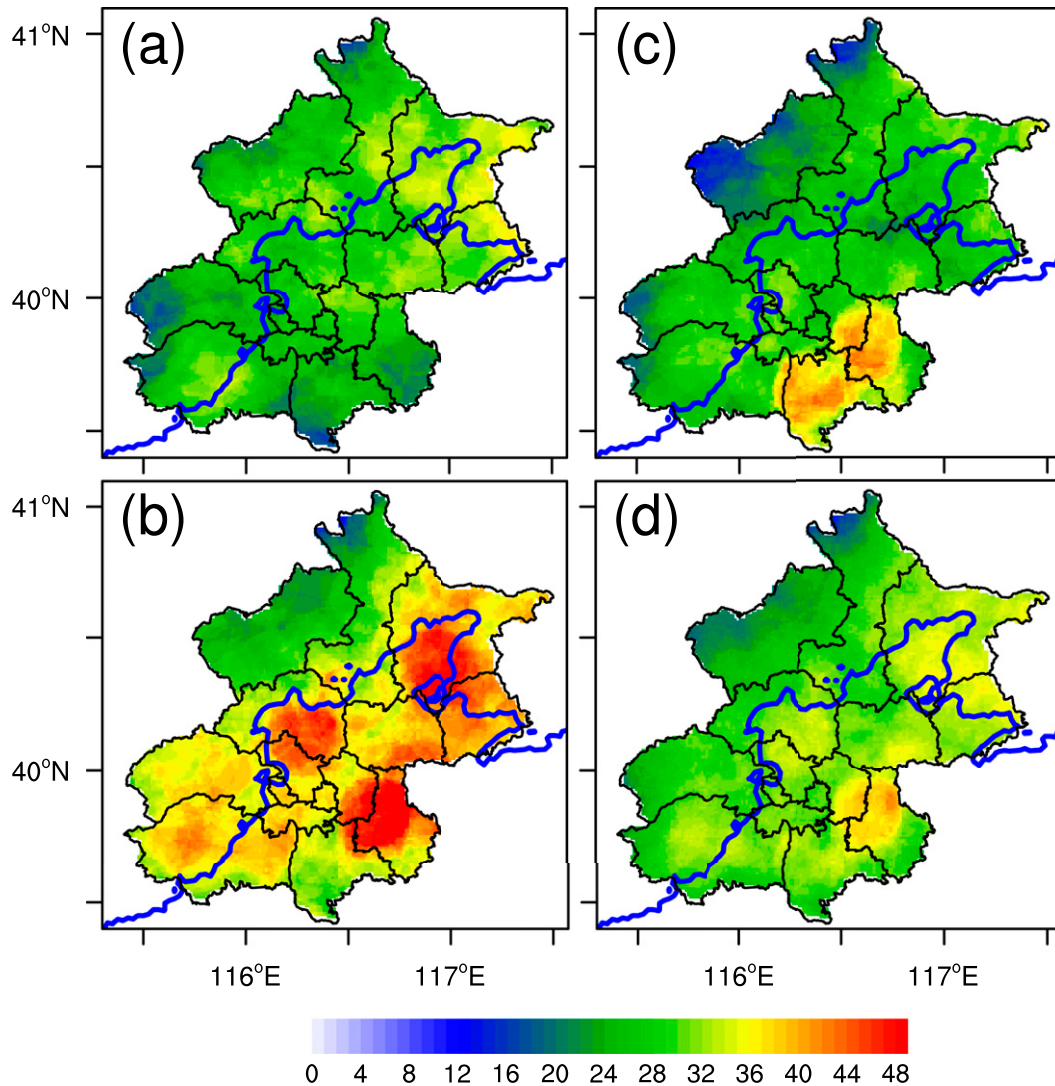
FIG. 14. Spatial distribution of annual lightning days for (a) 2005, (b) 2006, and (c) 2007 and (d) the 3-yr mean. Lightning days were calculated within a 15-km radius of each grid point with a 0.01° × 0.01° grid resolution over the BMR. The blue lines denote the 200-m terrain elevation.

located over the northeastern and southwestern mountainous areas (cf. Figs. 16b,c and 15d,e), while the lightning days with strong intensity (grades 4 and 5) were mostly located in the southeastern plains (cf. Figs. 16d,e and 15f,g), suggesting that thunderstorms propagating from the mountains to the plains were more directly related to intense lightning days.

f. Spatial variations in polarity characteristics and Z ratio

To facilitate comparisons with previous lightning studies, Fig. 17 shows the spatial variations in polarity characteristics and the Z ratio. Most positive CG flashes were distributed in the northeastern and southwestern

mountainous areas and in the southeastern plains with a maximum flash density of over 0.18 flashes per kilometer squared per year (Fig. 17a). Meanwhile, higher negative CG flash densities were mostly found in the southeastern plains with a maximum of over 1.50 flashes per kilometer squared per year (Fig. 17b), which was much greater than the positive CG flash densities. Both the spatial variations in positive and negative CG flash densities were significantly impacted by the detection efficiency. It is noted that the areas of higher values of negative CG flash densities were much smaller than that of positive CG flash densities. The reason mainly lies in that the decreasing detection efficiency of negative CG flashes was more significant than for positive ones.
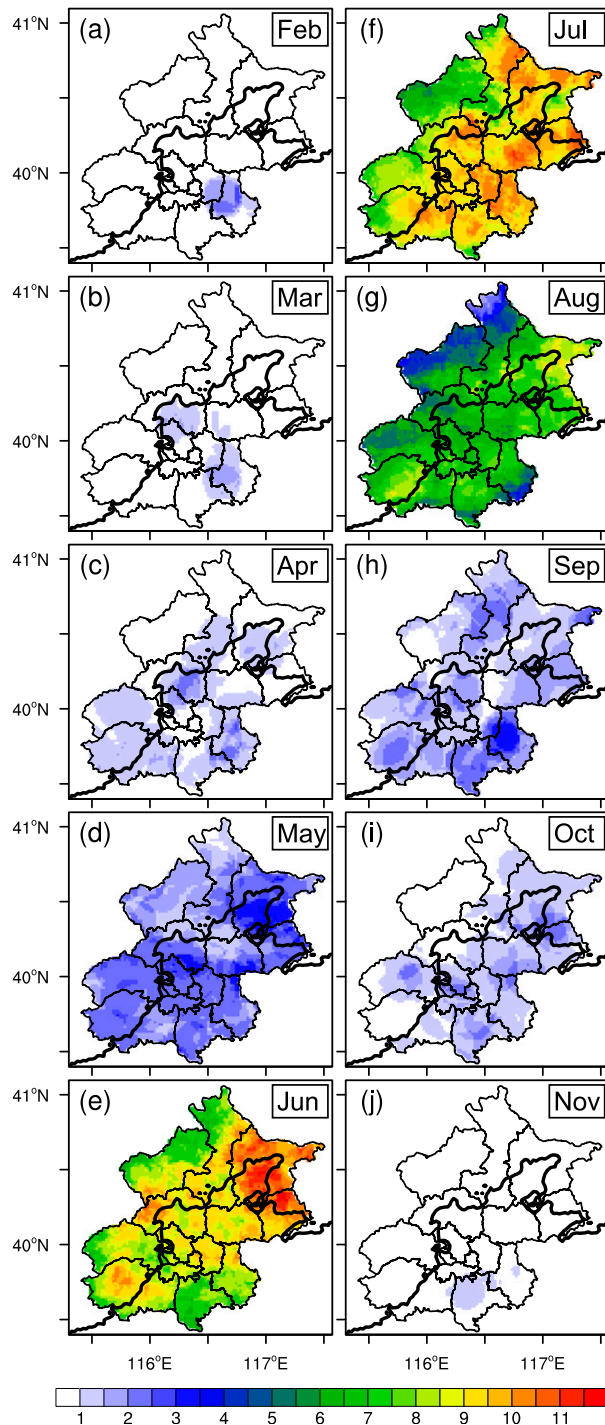
FIG. 15. Monthly spatial distribution of the lightning days (shaded) for the 3-yr period of 2005–07 over the BMR. Maps for January and December are not shown because of the absence of lightning days. Lightning days were calculated within a radius of 15 km from each grid point with a 0.01° × 0.01° grid resolution. The black thick lines denote the 200-m terrain elevation.
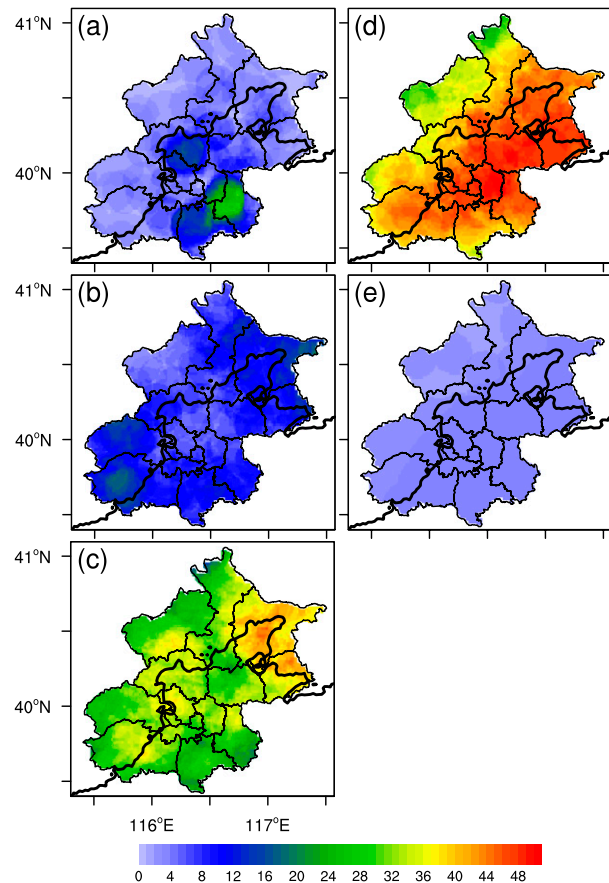

FIG. 16. Spatial distribution of lightning days with intensity grades (a) 1, (b) 2, (c) 3, (d) 4, and (e) 5 for the 3-yr period of 2005–07 over the BMR. Lightning days were calculated within a 15-km radius of each grid point with a 0.01° × 0.01° grid resolution. The thick black lines denote the 200-m terrain elevation.

Higher P_{PCG} values (greater than 15%) were found in the mountainous areas, especially over the northwestern mountains with a maximum of more than 40%, while P_{PCG} values of less than 15% were distributed in the plains (Fig. 17c). This pattern was opposite to the spatial variation of CG flashes, but the possible relationship between P_{PCG} and elevation is still uncertain. However, much higher values of P_{PCG} were seen over higher elevations, for example, more than 40% over the northern mountains. This is much greater than local high P_{PCG} anomalies found elsewhere, such as 10%–20% in the upper Midwest United States (Orville and Huffines 2001), more than 6% in the northeastern parts of Poland (Taszarek et al. 2015), and greater than 18% in northwestern China (Yang et al. 2015). Such a large P_{PCG} seems to be caused by the lower detection efficiency in the north of the BMR (Liu et al. 2013), as positive CG flashes usually have higher peak currents, thus are easier to detect than negative ones (Orville 1994). The distribution
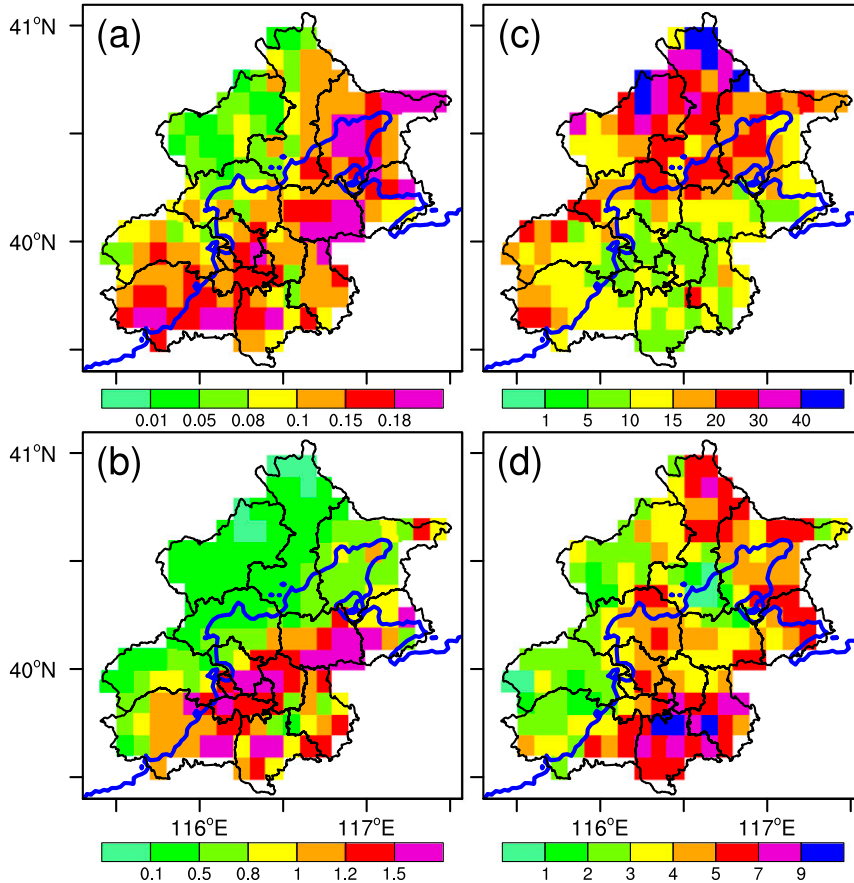
FIG. 17. Spatial distributions of the mean (a) PCG and (b) NCG flash densities (flashes per kilometer squared per year), (c) P_{PCG} (%), and (d) Z ratio on a $0.1° \times 0.1°$ grid resolution for the 3-yr period of 2005–07 over the BMR. The blue lines denote the 200-m terrain elevation.

of the Z ratio with a maximum in the southern plains is similar to the distribution of IC flash density, except for the large anomalies in the northern mountains (Fig. 17d), which is again attributed to the lower detection efficiency of CG flashes.

4. Summary and concluding remarks

In this study, we examined the CG and IC lightning characteristics over the BMR using data from the SAFIR-3000 lightning location system during the period of 2005–07. The lightning activity statistics, spatiotemporal variations and polarity characteristics, including the Z ratio, and lightning days with different intensities were analyzed. The topographic effects on the spatiotemporal features and polarity characteristics of lightning activity were also investigated. The main results are summarized below.

1) The 3-yr lightning statistics showed a total of 299 lightning days with 241 668 lightning flashes over the BMR, among which IC and CG flashes accounted for

81% and 19%, respectively. Negative CG flashes were more frequent than positive ones with a 3-yr-average P_{PCG} of 13.5%. A Z ratio of 4.38 was found over the BMR, which is much higher than that for the continental United States (2.64–2.94; Boccippio et al. 2001) and the Iberian Peninsula (3.48; Rivas Soriano and de Pablo 2007). This implies that IC flashes are more common over the BMR.

2) The monthly variations in lightning activity (both CG and IC) showed the largest contributions of flashes and high-intensity-grade lightning days during the summer months. Similar peak months of lightning activity were also found in other areas of the Yangtze River basin and southern China (Xia et al. 2015), the continental United States (Villarini and Smith 2013), Belgium (Poelman 2014), and Poland (Taszarek et al. 2015). In contrast, lightning days with lower intensity grades usually occurred during the spring and autumn months. Unlike P_{CG}, which showed a monthly variation similar to CG flashes, P_{PCG} exhibited an opposite trend, with higher values

occurring during the spring and autumn months and lower values during the summer months. The results also showed significant topographic effects on the monthly spatial variations in lightning density, with higher values on the northeastern and southwestern mountains during the spring months and over the southeastern plains during the summer months.

3) The diurnal variations in lightning activity showed a major peak around 1900 BST and a secondary peak around 2300 BST. An analysis of the diurnal spatial variation showed different diurnal peaks over the BMR's mountainous and plains regions: an afternoon peak on the northeastern and southwestern mountains and a night peak in the southeastern plains. This result is consistent with the diurnal variations in rainfall events and convective initiations over the BMR (Wang et al. 2014; Yuan et al. 2014), indicating the important roles of local topography in determining the lightning activity and convective weather. Moreover, an obvious negative correlation between P_{CG} and P_{PCG} and a positive correlation between P_{PCG} and the Z ratio were also found.

4) The spatial variations in flash density showed significant differences between the mountainous and plain areas. Although the mean CG and IC flash densities differed in magnitude, they all exhibited a southeastwardly increasing pattern from the northwestern mountains to the southeastern plains. Similarly, the lightning days also showed higher values in the southeastern plains and northeastern and southwestern mountains, and minimum values on the northwestern mountains. In addition, lightning activity on intense lightning days often occurred in the southeastern plains, while on weak lightning days it often occurred in the northeastern and southwestern mountainous regions. However, previous studies of CG lightning flashes over the BMR have shown that higher lightning densities are often distributed on the southwestern and northeastern mountains (Qie et al. 1991; He and Li 2005; Zheng et al. 2005; Zhou et al. 2009; R. Li et al. 2013). The results in this paper confirm the spatial distributions in previous studies, except for the higher lightning densities in the southeastern plains and lower densities in the northwestern mountains. The differences were perhaps caused by the deceasing detection efficiency from the southeastern plains to the northwestern mountains.

The detection efficiency decreased significantly with increasing distance from the center of the three substations, and the possible influence of inhomogeneity on the spatial variations in lightning characteristics should be discussed in this paper. The higher detection efficiency in the southeastern plains could cause more observed flashes, and the lower detection efficiency on the northwestern mountains could result in the detection of fewer flashes. Furthermore, the influence of decreasing detection efficiency differed between positive CG (PCG), negative CG (NCG), and IC flashes and may have induced the anomalous high P_{PCG} values and Z ratio in the southwestern and northern margins of the BMR, where the most significant reduction in detection efficiency appeared. To examine the distinct contrast in lightning densities on the southeastern plains and northwestern mountains, independent observations of hourly precipitation from automatic weather stations (AWS) and temperature of bright blackbody (TBB) from the *FY-2C* satellite (Chinese geostationary meteorological satellite of Fengyun series) were applied to compare the spatial variations with SAFIR-3000 lightning data. Previous studies have shown that lightning activity is more closely related to convective rainfall during the warm season (Petersen and Rutledge 1998; Tapia et al. 1998; Soula and Chauzy 2001). Therefore, only heavy-precipitation events with total amount of rainfall greater than $10 \, \mathrm{mm \, h^{-1}}$ (Miao et al. 2016) during the summer months of 2005–07 were examined to exclude the small rainfalls caused by stratiform clouds. It was also found that the climatological characteristics of convective storms denoted by TBB $\leq -52°C$ were consistent with those of lightning observations (Zheng et al. 2007). The results showed that the total amount of heavy rainfall was larger in the southwestern and northeastern mountains. In the southeastern plains (especially in the urban area), the rainfall amount was significantly larger than that in the northwestern mountains (Fig. 18a). Meanwhile the higher percentages of TBB $\leq -52°C$ were distributed in the northeastern mountains and southeastern plains, and the lowest percentages were in the northwestern mountains (Fig. 18b). The spatial variation of heavy rainfall amount and TBB $\leq -52°C$ verified that the difference between the lightning densities in the southeastern plains and northwestern mountains really existed even though they were impacted by the decreasing detection efficiency.

It is noted that the conclusions on the monthly variation only take into account a 3-yr period of lightning data, so they must be carefully drawn and compared with previous studies. The monthly peak flash counts of CG and IC during the summer months (June–August) found in this study are consistent with the results of previous studies in the BMR (He and Li 2005; J. Li et al. 2013; R. Li et al. 2013) and in other places, such as Romania (Antonescu and Burcea 2010), Belgium (Poelman 2014), and Poland (Taszarek et al. 2015).
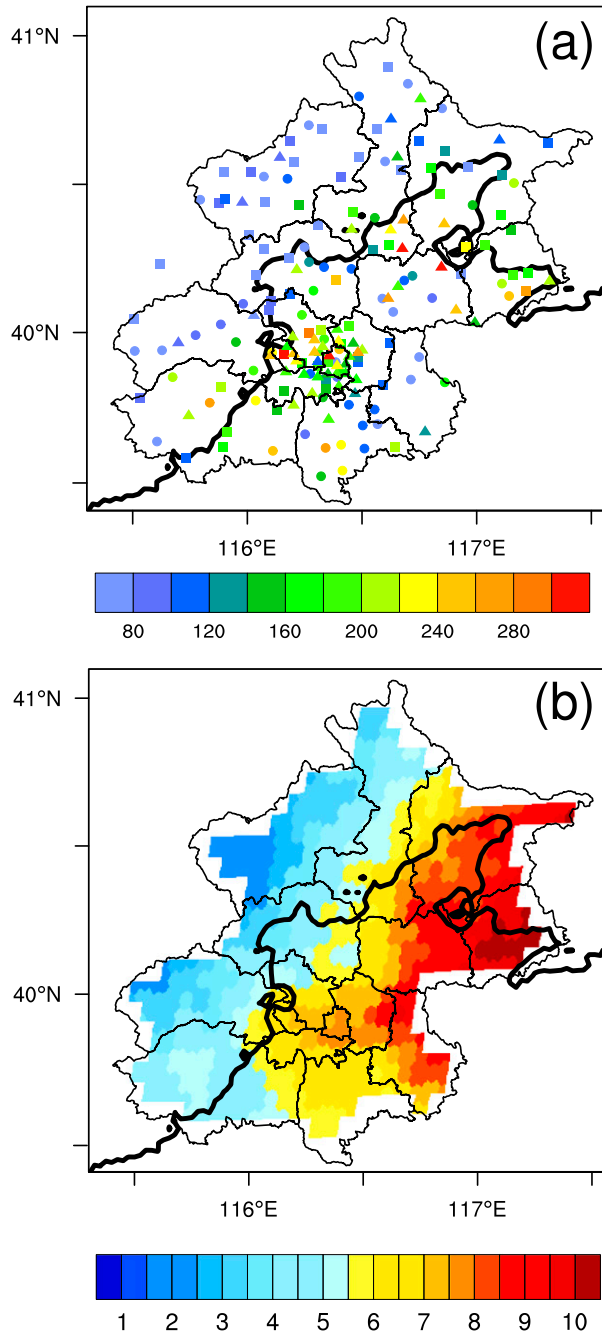
Therefore, although the study period was short, the conclusions on the monthly variations perhaps could reflect the monthly climatological map of lightning characteristics over the BMR. Meanwhile, the influence of individual lightning days with high lightning counts on the results of diurnal variations is negligible, as only the 3-yr data were included. The intense lightning days mainly caused the small diurnal peaks in the morning, and bimodal shapes of diurnal variations and more organized distributions of peak hourly IC flashes were found when the strong lightning days with intensity grade 5 were excluded (figure omitted).

The results obtained suggest that the SAFIR-3000 lightning detection system can be an effective tool in thunderstorm surveillance. Moreover, some recent studies have assimilated total lightning data into mesoscale numerical models to forecast severe storms (Fierro et al. 2012; Marchand and Fuelberg 2014). Thus, the SAFIR-3000 data could be more useful than CG flashes alone for improving model forecasts of severe storms over the BMR.

FIG. 18. (a) Spatial distribution of total rainfall amount (mm) of heavy-precipitation events ($\geq 10\,mm\,h^{-1}$) during 2005–07. Triangles, rectangles, and circles denote stations had precipitation observations starting from 2005, 2006, or 2007, respectively. (b) Spatial distribution of the percentage of hours with TBB $\leq$ $-52°C$ in the total heavy-precipitation events. Precipitation data are from the hourly observations of Beijing AWS, and TBB are from the *FY-2C* satellite hourly data with a resolution of $5\,km \times 5\,km$.

REFERENCES

Antonescu, B., and S. Burcea, 2010: A cloud-to-ground lightning climatology for Romania. *Mon. Wea. Rev.*, **138**, 579–591, doi:10.1175/2009MWR2975.1.

Beijing Municipal Bureau of Statistics, 2015: Yearly review (in Chinese). [Available online at http://www.bjstats.gov.cn/tjsj/cysj/201511/t20151109_311727.html.]

Boccippio, D. J., K. L. Cummins, H. J. Christian, and S. J. Goodman, 2001: Combined satellite- and surface-based estimation of the intracloud–cloud-to-ground lightning ratio over the continental United States. *Mon. Wea. Rev.*, **129**, 108–122, doi:10.1175/1520-0493(2001)129<0108:CSASBE>2.0.CO;2.

Bourscheidt, V., O. Pinto, K. P. Naccarato, and I. R. C. A. Pinto, 2009: The influence of topography on the cloud-to-ground lightning density in south Brazil. *Atmos. Res.*, **91**, 508–513, doi:10.1016/j.atmosres.2008.06.010.

Brook, M., M. Nakano, P. Krehbiel, and T. Takeuti, 1982: The electrical structure of the hokuriku winter thunderstorms. *J. Geophys. Res.*, **87**, 1207–1215, doi:10.1029/JC087iC02p01207.

Burrows, W. R., and B. Kochtubajda, 2010: A decade of cloud-to-ground lightning in Canada: 1999–2008. Part 1: Flash density and occurrence. *Atmos.–Ocean*, **48**, 177–194, doi:10.3137/AO1118.2010.

Carey, L. D., and S. A. Rutledge, 1998: Electrical and multiparameter radar observations of a severe hailstorm. *J. Geophys. Res.*, **103**, 13 979–14 000, doi:10.1029/97JD02626.

Chen, S., Y. Wang, W. Zhang, and M. Chen, 2011: Intensifying mechanism of the convective storm moving from the mountain to the plain over Beijing area. *Meteor. Mon.*, **37**, 802–813.

Chronis, T., L. D. Carey, C. J. Schultz, E. V. Schultz, K. M. Calhoun, and S. J. Goodman, 2015: Exploring lightning jump characteristics. *Wea. Forecasting*, **30**, 23–37, doi:10.1175/WAF-D-14-00064.1.

Cummins, K. L., 2014: Mapping the impact of terrain on lightning incidence and multiple ground contacts in cloud-to-ground flashes. *Proc. 15th Int. Conf. on Atmospheric Electricity*, Norman, OK, IUGG/IAMAS International Commission on Atmospheric Electricity. [Available online at http://www.nssl.noaa.gov/users/mansell/icae2014/preprints/Cummins_68.pdf.]

Czernecki, B., M. Taszarek, L. Kolendowicz, and J. Konarski, 2016: Relationship between human observations of thunderstorms and the PERUN lightning detection network in Poland. *Atmos. Res.*, **167**, 118–128, doi:10.1016/j.atmosres.2015.08.003.

Engholm, C. D., E. R. Williams, and R. M. Dole, 1990: Meteorological and electrical conditions associated with positive cloud-to-ground lightning. *Mon. Wea. Rev.*, **118**, 470–487, doi:10.1175/1520-0493(1990)118<0470:MAECAW>2.0.CO;2.

Enno, S. E., 2015: Comparison of thunderstorm hours registered by the lightning detection network and human observers in Estonia, 2006–2011. *Theor. Appl. Climatol.*, **121**, 13–22, doi:10.1007/s00704-014-1218-8.

Fierro, A. O., E. R. Mansell, C. L. Ziegler, and D. R. MacGorman, 2012: Application of a lightning data assimilation technique in the WRF-ARW Model at cloud-resolving scales for the tornado outbreak of 24 May 2011. *Mon. Wea. Rev.*, **140**, 2609–2627, doi:10.1175/MWR-D-11-00299.1.

Gao, L., 2009: To evaluate the detection ability of lightning location system via "concentric circles method" (in Chinese). *Central China Electric Power*, **22**, 26–29.

He, H., and H. Li, 2005: Preliminary analysis of lightning characteristics in Beijing (in Chinese). *Meteor. Sci. Tech.*, **33**, 496–500.

Huang, R., Y. Wang, and W. Zhang, 2012: Initiating and intensifying mechanism of a local thunderstorm over complex terrain of Beijing (in Chinese). *Torrential Rain Disasters*, **31**, 232–241.

Kotroni, V., and K. Lagouvardos, 2008: Lightning occurrence in relation with elevation, terrain slope, and vegetation cover in the Mediterranean. *J. Geophys. Res.*, **113**, D21118, doi:10.1029/2008JD010605.

Li, J., R. Yu, and J. Wang, 2008: Diurnal variations of summer precipitation in Beijing (in Chinese). *Chin. Sci. Bull.*, **53**, 1933–1936.

——, H. Song, W. Xiao, X. Du, and F. Guo, 2013: Temporal-spatial characteristics of lightning over Beijing and its circumjacent regions (in Chinese). *Trans. Atmos. Sci.*, **36**, 235–245.

Li, R., X. Lu, H. Zhang, J. Li, and Y. Zhang, 2013: Temporal and spatial distribution characteristics of cloud-to-ground flash from 2008 to 2010 in Beijing (in Chinese). *Meteor. Environ. Sci.*, **36**, 52–56.

Liou, Y. A., and S. K. Kar, 2010: Study of cloud-to-ground lightning and precipitation and their seasonal and geographical characteristics over Taiwan. *Atmos. Res.*, **95**, 115–122, doi:10.1016/j.atmosres.2009.08.016.

Liu, D., X. Qie, Y. Xiong, and G. Feng, 2011: Evolution of the total lightning activity in a leading-line and trailing stratiform mesoscale convective system over Beijing. *Adv. Atmos. Sci.*, **28**, 866–878, doi:10.1007/s00376-010-0001-8.

——, ——, L. Pan, and L. Peng, 2013: Some characteristics of lightning activity and radiation source distribution in a squall line over north China. *Atmos. Res.*, **132–133**, 423–433, doi:10.1016/j.atmosres.2013.06.010.

MacGorman, D. R., and D. W. Burgess, 1994: Positive cloud-to-ground lightning in tornadic storms and hailstorms. *Mon. Wea. Rev.*, **122**, 1671–1697, doi:10.1175/1520-0493(1994)122<1671:PCTGLI>2.0.CO;2.

——, ——, V. Mazur, W. D. Rust, W. L. Taylor, and B. C. Johnson, 1989: Lightning rates relative to tornadic storm evolution on 22 May 1981. *J. Atmos. Sci.*, **46**, 221–251, doi:10.1175/1520-0469(1989)046<0221:LRRTTS>2.0.CO;2.

Marchand, M. R., and H. E. Fuelberg, 2014: Assimilation of lightning data using a nudging method involving low-level warming. *Mon. Wea. Rev.*, **142**, 4850–4871, doi:10.1175/MWR-D-14-00076.1.

Miao, C., Q. Sun, A. G. Borthwick, and Q. Duan, 2016: Linkage between hourly precipitation events and atmospheric temperature changes over China during the warm season. *Sci. Rep.*, **6**, 22543, doi:10.1038/srep22543.

Naccarato, K., O. Pinto, and I. Pinto, 2003: Evidence of thermal and aerosol effects on the cloud-to-ground lightning density and polarity over large urban areas of southeastern Brazil. *Geophys. Res. Lett.*, **30**, 1674, doi:10.1029/2003GL017496.

Nishihashi, M., K.-I. Arai, C. Fujiwara, W. Mashiko, S. Yoshida, S. Hayashi, and K. Kusunoki, 2015: Characteristics of lightning jumps associated with a tornadic supercell on 2 September 2013. *SOLA*, **11**, 18–22, doi:10.2151/sola.2015-005.

Novák, P., and H. Kyznarová, 2011: Climatology of lightning in the Czech Republic. *Atmos. Res.*, **100**, 318–333, doi:10.1016/j.atmosres.2010.08.022.

Orville, R. E., 1994: Cloud-to-ground lightning flash characteristics in the contiguous United States: 1989–1991. *J. Geophys. Res.*, **99**, 10 833–10 841, doi:10.1029/93JD02914.

——, and G. R. Huffines, 2001: Cloud-to-ground lightning in the United States: NLDN results in the first decade, 1989–98. *Mon. Wea. Rev.*, **129**, 1179–1193, doi:10.1175/1520-0493(2001)129<1179:CTGLIT>2.0.CO;2.

Petersen, W. A., and S. A. Rutledge, 1998: On the relationship between cloud-to-ground lightning and convective rainfall. *J. Geophys. Res.*, **103**, 14 025–14 040, doi:10.1029/97JD02064.

Pinto, O., I. Pinto, and H. de Faria, 2003: A comparative analysis of lightning data from lightning networks and LIS sensor in the north and southeast of Brazil. *Geophys. Res. Lett.*, **30**, 1073, doi:10.1029/2002GL016009.

Poelman, D. R., 2014: A 10-year study on the characteristics of thunderstorms in Belgium based on cloud-to-ground lightning data. *Mon. Wea. Rev.*, **142**, 4839–4849, doi:10.1175/MWR-D-14-00202.1.

Price, C., and D. Rind, 1993: What determines the cloud-to-ground lightning fraction in thunderstorms? *Geophys. Res. Lett.*, **20**, 463–466, doi:10.1029/93GL00226.

Qie, X., C. Guo, and X. Liu, 1991: The characteristics of ground flashes in Beijing and Lanzhou regions. *Adv. Atmos. Sci.*, **8**, 471–478, doi:10.1007/BF02919269.

——, Y. Yu, D. Wang, H. Wang, and R. Chu, 2002: Characteristics of cloud-to-ground lightning in Chinese inland

plateau. *J. Meteor. Soc. Japan*, **80**, 745–754, doi:10.2151/jmsj.80.745.

Rakov, V. A., and M. A. Uman, 2003: *Lightning: Physics and Effects.* Cambridge University Press, 698 pp.

Rivas Soriano, L., and F. de Pablo, 2007: Total flash density and the intracloud/cloud-to-ground lightning ratio over the Iberian Peninsula. *J. Geophys. Res.*, **112**, D13114, doi:10.1029/2006JD007624.

——, ——, and C. Tomas, 2005: Ten-year study of cloud-to-ground lightning activity in the Iberian Peninsula. *J. Atmos. Sol. Terr. Phys.*, **67**, 1632–1639, doi:10.1016/j.jastp.2005.08.019.

Schultz, C. J., W. A. Petersen, and L. D. Carey, 2011: Lightning and severe weather: A comparison between total and cloud-to-ground lightning trends. *Wea. Forecasting*, **26**, 744–755, doi:10.1175/WAF-D-10-05026.1.

——, L. D. Carey, E. V. Schultz, and R. J. Blakeslee, 2015: Insight into the kinematic and microphysical processes that control lightning jumps. *Wea. Forecasting*, **30**, 1591–1621, doi:10.1175/WAF-D-14-00147.1.

Schulz, W., K. Cummins, G. Diendorfer, and M. Dorninger, 2005: Cloud-to-ground lightning in Austria: A 10-year study using data from a lightning location system. *J. Geophys. Res.*, **110**, D09101, doi:10.1029/2004JD005332.

Soula, S., and S. Chauzy, 2001: Some aspects of the correlation between lightning and rain activities in thunderstorms. *Atmos. Res.*, **56**, 355–373, doi:10.1016/S0169-8095(00)00086-7.

Takeuti, T., M. Nakano, M. Brook, D. J. Raymond, and P. Krehbiel, 1978: The anomalous winter thunderstorms of the Hokuriku Coast. *J. Geophys. Res.*, **83**, 2385–2394, doi:10.1029/JC083iC05p02385.

Tapia, A., J. A. Smith, and M. Dixon, 1998: Estimation of convective rainfall from lightning observations. *J. Appl. Meteor.*, **37**, 1497–1509, doi:10.1175/1520-0450(1998)037<1497:EOCRFL>2.0.CO;2.

Taszarek, M., B. Czernecki, and A. Kozioł, 2015: A cloud-to-ground lightning climatology for Poland. *Mon. Wea. Rev.*, **143**, 4285–4304, doi:10.1175/MWR-D-15-0206.1.

Villarini, G., and J. A. Smith, 2013: Spatial and temporal variability of cloud-to-ground lightning over the continental U.S. during the period 1995–2010. *Atmos. Res.*, **124**, 137–148, doi:10.1016/j.atmosres.2012.12.017.

Vogt, B. J., and S. J. Hodanish, 2014: A high-resolution lightning map of the state of Colorado. *Mon. Wea. Rev.*, **142**, 2353–2360, doi:10.1175/MWR-D-13-00334.1.

Wang, Y., L. Han, and H. Wang, 2014: Statistical characteristics of convective initiation in the Beijing-Tianjin region revealed by six-year radar data. *J. Meteor. Res.*, **28**, 1127–1136, doi:10.1007/s13351-014-3061-3.

Wiens, K. C., S. A. Rutledge, and S. A. Tessendorf, 2005: The 29 June 2000 supercell observed during STEPS. Part II: Lightning and charge structure. *J. Atmos. Sci.*, **62**, 4151–4177, doi:10.1175/JAS3615.1.

Williams, E., M. Weber, and R. Orville, 1989: The relationship between lightning type and convective state of thunderclouds. *J. Geophys. Res.*, **94**, 13 213–13 220, doi:10.1029/JD094iD11p13213.

Xia, R., D.-L. Zhang, and B. Wang, 2015: A 6-yr cloud-to-ground lightning climatology and its relationship to rainfall over central and eastern China. *J. Appl. Meteor. Climatol.*, **54**, 2442–2460, doi:10.1175/JAMC-D-15-0029.1.

Xue, Q., Q. Meng, and R. Ge, 1999: The relationship between lightning activity and severe convection weather in Beijing area in summer from 1995 to 1997 (in Chinese). *Meteor. Mon.*, **25**, 15–19.

Yang, P., G. Ren, W. Hou, and W. Liu, 2013: Spatial and diurnal characteristics of summer rainfall over Beijing municipality based on a high-density AWS dataset. *Int. J. Climatol.*, **33**, 2769–2780, doi:10.1002/joc.3622.

Yang, X., J. Sun, and W. Li, 2015: An analysis of cloud-to-ground lightning in China during 2010–13. *Wea. Forecasting*, **30**, 1537–1550, doi:10.1175/WAF-D-14-00132.1.

Yin, S., W. Li, D. Chen, J.-H. Jeong, and W. Guo, 2011: Diurnal variations of summer precipitation in the Beijing area and the possible effect of topography and urbanization. *Adv. Atmos. Sci.*, **28**, 725–734, doi:10.1007/s00376-010-9240-y.

Yuan, W., W. Sun, H. Chen, and R. Yu, 2014: Topographic effects on spatiotemporal variations of short-duration rainfall events in warm season of central north China. *J. Geophys. Res.*, **119**, 11 223–11 234, doi:10.1002/2014JD022073.

Zhang, W., Q. Meng, M. Ma, and Y. Zhang, 2011: Lightning casualties and damages in China from 1997 to 2009. *Nat. Hazards*, **57**, 465–476, doi:10.1007/s11069-010-9628-0.

Zheng, D., Q. Meng, W. Lü, Y. Zhang, X. Cai, and M. Ma, 2005: Spatial and temporal characteristics of cloud-to-ground lightning in summer in Beijing and its circumjacent regions (in Chinese). *Chin. J. Appl. Meteor.*, **16**, 638–644.

——, Y. Zhang, Q. Meng, W. Lü, and X. Yi, 2009: Total lightning characteristics and electric structure evolution in a hailstorm. *Acta Meteor. Sin.*, **23**, 233–249.

Zheng, Y., J. Chen, M. Chen, Y. Wang, and Q. Ding, 2007: Statistic characteristics and weather significance of infrared TBB during May–August in Beijing and its vicinity. *Chin. Sci. Bull.*, **52**, 3428–3435, doi:10.1007/s11434-007-0438-z.

Zhou, Y., J. Zhang, and L. Sun, 2009: Statistic analysis on cloud-to-ground lightning characteristics over Beijing, Tianjin and Hebei Province. *J. Catastrophol.*, **24**, 101–105.